Check for updates

Design strategy and mechanism of nitrite oxidation suppression of elevated loading rate partial nitritation system

Juliet Ikem, Huiyu Chen and Robert Delatolla*

Department of Civil Engineering, Ottawa-Carleton Institute for Environmental Engineering, University of Ottawa, Ottawa, ON, Canada

There is a current need for a low operational intensity, effective and small footprint system to achieve stable partial nitration for subsequent anammox treatment at mainstream municipal wastewaters. This research identifies a unique design strategy using an elevated total ammonia nitrogen (TAN) surface area loading rate (SALR) of 5g TAN/m^2·d to achieve cost-effective, stable, and elevated rates of partial nitration in a moving bed biofilm reactor (MBBR) system under mainstream conditions. The elevated loaded partial nitration MBBR system achieves a TAN surface area removal rate (SARR) of 2.01 ± 0.07g TAN/m^2·d and NO_2^--N: NH_4^+-N stoichiometric ratio of 1.15:1, which is appropriate for downstream anammox treatment. The elevated TAN SALR design strategy promotes nitrite-oxidizing bacteria (NOB) activity suppression rather than a reduction in NOB population as the reason for the suppression of nitrite oxidation in the mainstream elevated loaded partial nitration MBBR system. NOB activity is limited at an elevated TAN SALR likely due to thick biofilm embedding the NOB population and competition for dissolved oxygen (DO) with ammonia-oxidizing bacteria for TAN oxidation to nitrite within the biofilm structure, which ultimately limits the uptake of DO by NOB in the system. Therefore, this design strategy offers a cost-effective and efficient alternative for mainstream partial nitration MBBR systems at water resource recovery facilities.

KEYWORDS

municipal wastewater, ammonia removal, anammox, moving bed biofilm reactor, nitrite oxidation suppression, mainstream

1. Introduction

Partial nitration and anaerobic ammonia oxidation (anammox), known as the PN/A process, is an autotrophic nitrogen removal process based on two consecutive processes: ammonia-oxidizing bacteria (AOB) oxidizing about 55% of the total ammonia nitrogen (TAN) to nitrite, and subsequently, anammox bacteria (AnAOB) converting the produced nitrite and residual TAN to nitrogen gas with limited nitrate production. Compared to conventional nitrification and denitrification, PN/A is more cost-effective and energy-efficient and could significantly reduce the energy consumption of water resource recovery facilities (WRRFs) by 20–40% (Agrawal et al., 2018; Pedrouso et al., 2019). Over the past decade, the PN/A process has been successfully implemented to treat sludge digester centrate, also termed "sidestream wastewaters," within municipal WRRFs (Lackner et al., 2014; Lotti et al., 2015b). In recent years, there has been renewed interest in exploring the PN/A process at conditions more typical

for mainstream municipal wastewater. However, mainstream municipal wastewaters are characterized by low TAN concentrations (20–40 mg TAN/L), high C/N ratios (7–12 g COD/g-N), variable TAN loading rates, and low temperatures (<10°C), with these characteristics limiting the successful implementation of the PN/A process at WRRFs. These mainstream wastewater characteristics have been demonstrated to limit AOB and AnAOB growth rates and also increase the challenge of achieving effective nitrite oxidation suppression; which is necessary to maintain ideal effluent quality and long-term process stability in mainstream PN/A systems (Gilbert et al., 2015; Li et al., 2018; Hoekstra et al., 2019).

Long-term nitrite oxidation suppression in mainstream PN/A systems has been investigated using a one-stage system, where partial nitritation and anammox occur in the same reactor, or a two-stage system with partial nitritation and anammox occurring in separate reactors (Laureni et al., 2016; Chen et al., 2018; Gu et al., 2018; Gustavsson et al., 2020; Schraa et al., 2020; Trojanowicz et al., 2021; Choi and Jung, 2022). While the one-stage configured systems are mostly studied due to the lower cost of infrastructure than two-stage configured systems, the latter offers the opportunity to optimize the stable partial nitritation and anammox process independently and maintain a balanced ratio between functional bacteria groups (AOB and AnAOB) to achieve higher volumetric nitrogen removal rates.

In a two-stage configured system, optimization of the partial nitritation process requires effective operational control strategies to ensure that the nitrite-oxidizing bacteria (NOB) population or activity is continuously suppressed within the system (Piculell et al., 2016a; Gu et al., 2018; Choi and Jung, 2022). In this regard, several operational control strategies have been employed in a two-stage configured system involving either suspended growth or attached growth systems to achieve stable partial nitritation. Recently, research has focused on hybrid system where attached growth biofilms and flocs coexist, also known as integrated fixed-film activated sludge (IFAS) systems, and biofilm technologies such as the moving bed biofilm reactor (MBBR) system (Laureni et al., 2016, 2019; Gu et al., 2018; Kowalski et al., 2019a; Gustavsson et al., 2020; Trojanowicz et al., 2021). Recent interest in biofilm technologies is due to their ability to retain highly specialized microbial populations and also because biofilm structure results in substrate gradients that can promote suppression of the growth of the NOB population or suppression of the NOB activity (Brockmann and Morgenroth, 2008; Gilbert et al., 2014; Pérez et al., 2014; Lotti et al., 2015a; Piculell et al., 2016a).

Several operational control strategies have been applied using the MBBR technology to selectively inhibit NOB population or activity (Lotti et al., 2014; Pérez et al., 2014; Gilbert et al., 2015; Laureni et al., 2016). Some of the operational control strategies that have been reported in mainstream partial nitritation two-stage MBBR systems include: alternating feed from sidestream to mainstream; bioaugmentating with AOB biomass; controlling biofilm thickness; exposure of biomass to toxic sidestream effluent or conditions favorable for AOB growth; employing a combination of dissolved oxygen (DO)/TAN ratio control and free ammonia (FA) inhibition; and alternating anoxic and aerobic condition through intermittent aeration (Piculell et al., 2016a,b; Gu et al., 2018; Kowalski et al., 2019a,b). Notwithstanding the potential of NOB suppression using these operational control strategies, these strategies are all operationally intensive and have demonstrated difficulty in achieving long-term suppression of NOB population or activity, overall process stability, and stable effluent quality.

In recent studies, an elevated TAN loading rate, as a means of a passive and low operational design strategy, has been shown to achieve stable partial nitritation rates within a two-stage configured MBBR system (Schopf et al., 2019, 2021; Ikem et al., 2023). Schopf et al. (2019, 2021) achieved stable and robust partial nitritation at an elevated TAN loading rate of 6.5 g TAN/m²·d in an MBBR system fed with TAN concentration of 125mg TAN/L, simulating TAN concentrations observed in industrial wastewaters. In this system, stable partial nitritation was attributed to the morphological impacts resulting from operating at an elevated TAN loading rate that could allow for NOB activity to be effectively suppressed (Schopf et al., 2021). Consequently, the feasibility of using this design strategy to achieve stable partial nitritation has been evaluated at conditions and TAN concentrations between 25 to 44 mg TAN/L typical for mainstream municipal wastewater (Ikem et al., 2023). Ikem et al. identified critical design parameters, a TAN surface area loading rate (SALR), a hydraulic retention time (HRT), and an airflow rate optimized for stable partial nitritation of a mainstream elevated loaded MBBR system. However, this system did not achieve the ideal effluent NO_2^--N:NH_4^+-N stoichiometric ratio of 1.31:1 for subsequent anammox treatment. Specifically, the average NO_2^--N:NH_4^+-N stoichiometric ratio reported in this study was at 0.70:1, which is not comparable to the optimized ratio proposed by Strous et al. (1998) for anammox operation. The operation of anammox system with inappropriate effluent stoichiometric ratio from the partial nitritation system has been demonstrated to impact the attachment and enrichment of anammox cells in a full-scale MBBR, leading to process instability (Stefansdottir et al., 2015). Hence, further optimization of the elevated loaded partial nitritation MBBR system is required to improve effluent quality for downstream anammox operation. Moreover, further investigation of biofilm characteristics, embedded cells, and microbiome response is needed to understand nitrite oxidation suppression mechanism responsible for stable partial nitritation of mainstream elevated loaded MBBR systems. Although previous work has investigated the mechanism and method of nitrite oxidation suppression caused by employing elevated TAN loading rate for partial nitritation control, these studies were performed at higher influent TAN concentrations not typically observed in mainstream municipal wastewater (Schopf et al., 2019, 2021). Thus, there is a significant knowledge gap and a need to investigate further the mechanism of nitrite oxidation suppression in the elevated loaded partial nitritation system that would ensure high performance and long-term operational stability under mainstream conditions.

Therefore, this study aims to identify the mechanism of nitrite oxidation suppression of mainstream elevated loaded partial nitritation MBBR systems. The specific objectives were to (i) characterize the performance of a two-reactor in series designed mainstream elevated loaded partial nitritation MBBR system; (ii) determine the effects of elevated TAN loading rate on biofilm thickness, biofilm mass, biofilm density, and embedded cells, and how these characteristics influence the performance of the mainstream partial nitritation MBBR system; and (iii) quantitate the AOB and NOB population counts within the attached growth, biofilm community and identify whether NOB population suppression or NOB activity suppression is responsible for partial nitritation.

2. Materials and methods

2.1. Reactor configuration and operation

Two-reactors in series partial nitritation MBBR system configuration were identified in the preliminary work of this study based on findings from Ikem et al. (2023) to optimize the effluent concentration from the partial nitritation MBBR system for subsequent downstream anammox treatment. The experimental set-up consisted of two identical lab-scale MBBR reactors (2 L each) operated in series (Figure 1). The reactors were filled with high-density polyethylene AnoxK™5 carriers (AnoxKaldnes, Lund, Sweden) with a diameter of 25 mm, height of 4 mm, and bulk surface area of 800 m²/m³. The AnoxK™5 were seeded carriers harvested from a biological oxygen demand (BOD) removal municipal IFAS wastewater treatment system located in Hawkesbury, Ontario, Canada, and were operated in a single bench lab partial nitritation MBBR system operated at elevated TAN concentrations prior to this study. The reactors were designed at a target TAN SALR of 5 g TAN/m²·d, recommended as the optimum for the partial nitritation MBBR system based on the previous findings, as it demonstrated stable and steady performance as well as high partial nitritation rate (Schopf et al., 2019; Ikem et al., 2023). The TAN SALR in the nitrifying MBBR systems at ambient temperature are conventionally designed typically between 0.45 to 1.0 g TAN/m²·d with respect to target effluent TAN concentrations (Hem et al., 1994; Odegaard, 1999; Young et al., 2017b); thus, the TAN SALR present in this study was significantly elevated (referred to as elevated TAN SALR) than conventional TAN SALR which would potentially allow operating high-rate partial nitritation and small land footprint system. The elevated TAN SALR of 5 g TAN/m²·d in the partial nitritation reactors was achieved at mainstream concentrations through operation at relatively short target HRT of 2 h and low carrier fill fraction, at 6 and 9.5%. The first reactor, denoted P_{N1}, contained 39 carriers, and the second reactor P_{N2}, contained 28 carriers. The carriers accounted for 9.5 and 6% of the

total reactor volume, respectively. These different fractions were necessary to operate both reactors at similar elevated TAN SALR values of 5 g TAN/m²·d, as P_{N2} was fed with the effluent of P_{N1} and hence required fewer carriers to achieve the same SALR as P_{N1}. For clarity and easy understanding of this manuscript, the reactors in a series of P_{N1} and P_{N2} will be referred to as P_{N1-N2}.

P_{N1} and P_{N2} were both equipped with a coarse bubble aeration system, with diffusers positioned at the base of the reactors to provide adequate DO in the bulk solution and allow sufficient mixing of the carriers. The airflow rates were maintained at 1.5 and 1 L/min for P_{N1} and P_{N2}, respectively, as previous findings demonstrated that adjusting airflow above 1.5 L/min resulted in increased nitrite oxidation to nitrate (Ikem et al., 2023). Moreover, P_{N2} had lower influent TAN concentration and fewer carriers than P_{N1}; as such would necessitate a reduced airflow rate to limit nitrite oxidation. P_{N1} was fed with a peristaltic pump with influent from a wastewater feed tank, and P_{N2} was fed *via* gravitational flow with the effluent from P_{N1}. The target (measured) influent TAN concentrations were 30 (32.16 ± 0.46) mg TAN/L for P_{N1} and 20 (20.4 ± 1.54) mg TAN/L for P_{N2}, all within the conventional limits of mainstream municipal TAN concentrations. The operational conditions for both reactors were the same with the following target (measured) values: SALR of 5 (5.07 ± 0.22) g TAN/m²·d, HRT of 2 (2.02 ± 0.02) h, DO of 6.5 (6.84 ± 0.05) mg O₂/L, pH of 7.5 (7.76 ± 0.05), and temperature 20 (19.9 ± 0.10)°C.

2.2. Wastewater feed

Synthetic wastewater (SWW) was prepared based on a recipe from previous studies (Delatolla et al., 2009; Schopf et al., 2019; Tian et al., 2019). The SWW simulated wastewater effluent from a carbon removal process without TAN removal and was composed as follows (per L of SWW): 0.14 g $(NH_4^+)_2SO_4$ (corresponding to a concentration of approximately 30 mg NH_4^+-N/L), 0.39 g $NaHCO_3$, 0.06 g $MgSO_4 \cdot 7H_2O$, 0.02 g $CaCl_2 \cdot 2H_2O$, 0.06 g KH_2PO_4, and 0.004 g

FIGURE 1
Experimental set-up.
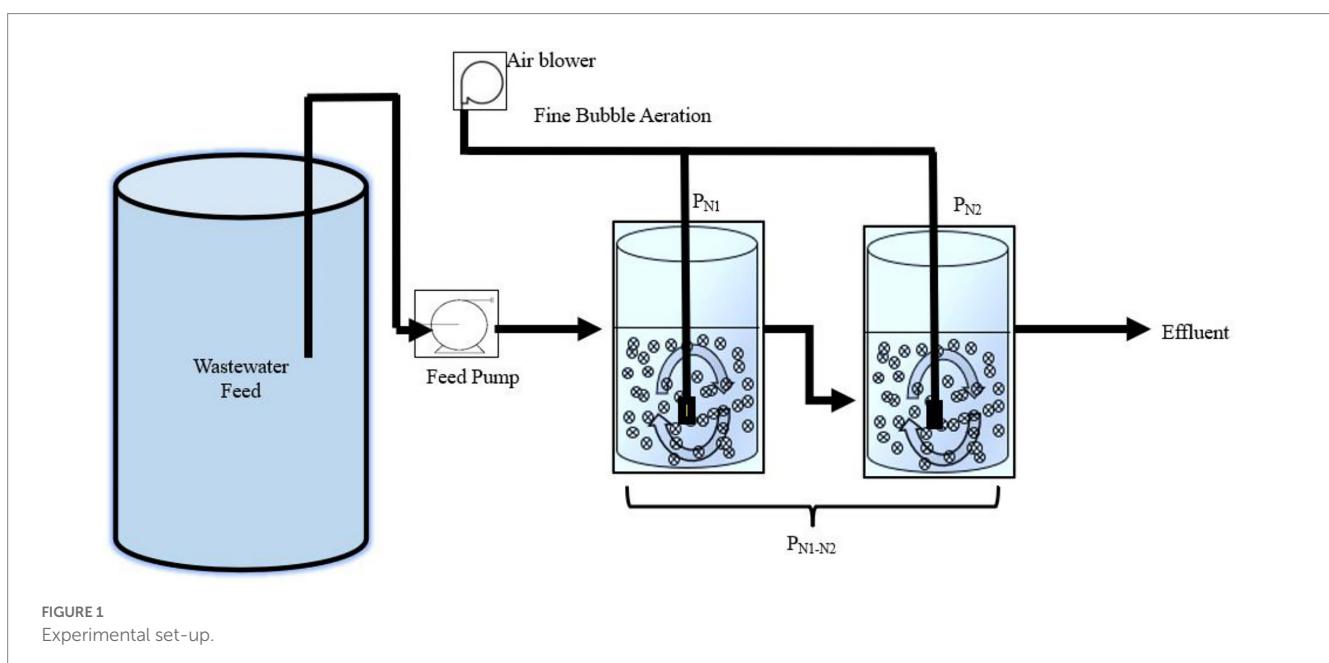
$FeSO_4 \cdot 7H_2O$. Trace nutrients (per L of SWW) included: $MnCl_2 \cdot 4H_2O$: 0.10 mg, $Na_2MoO_4 \cdot 2H_2O$: 0.03 mg, $CuSO_4 \cdot 5H_2O$: 0.10 mg, $CoCl_2 \cdot 6H_2O$: 0.001 mg, and $ZnSO_4 \cdot 7H_2O$: 0.03 mg. The carbon source composition (per L of synthetic wastewater): glucose 4.86 mg, sodium acetate 2.59 mg, and peptone 4.86 mg resulted in a sCOD concentration of 25 mg sCOD/L, thereby mimicking post-carbon effluent (Schopf et al., 2019).

2.3. Constituent analyses

Wastewater constituent analyses were performed on each of the two MBBR reactors in series, P_{N1} and P_{N2}. Wastewater samples were collected three times a week from both reactors for analyses, and the samples were tested in triplicate for the following parameters: TAN, nitrite, nitrate, DO, sCOD, pH, temperature, alkalinity, total suspended solids (TSS), and volatile suspended solids (VSS). To quantify the kinetics of the reactors, the following standard methods were used: Nessler-4500C-NH_3, 4500B-NO_2^- and nitrate 4500A-NO_3^- for TAN, nitrite, and nitrate, respectively. DO and temperature measurements were acquired using a HACH Flexi HQ30d DO/temperature probe (HACH, Loveland, CO, United States) and pH was measured using a SympHony VWR pH probe (VWR, Ontario, Canada). sCOD was quantified using a HACH 8000 (HACH, Loveland, CO, United States), and TSS and VSS were measured using standard methods 2540D (Clesceri et al., 1999). In addition, the aeration rates were monitored and measured using a Dwyer VFA-24 Visi-Float® acrylic airflow meter (DWYER, Michigan City, IN, USA).

2.4. Biofilm morphology, thickness, and mass

Stereomicroscopy was used to acquire images of *in-situ* biofilm thickness and morphology. Stereomicroscopy was used because it does not require any sample preparation as such maximizes the integrity of the sample and artifact creation. Four carriers per reactor were extracted and analyzed within 4 h of being harvested. Five images per carrier were acquired at ×2 magnification and were used to determine biofilm thickness. Also, one image per carrier was acquired and analyzed at ×4 magnification to assess the biofilm surface morphology. All of these images were taken at random locations across the carrier surface to avoid bias. Finally, two images per carrier were obtained at ×0.8 magnification to verify biofilm attachment across the carriers. The biofilm thicknesses were quantified using ImageJ 1.52a image processing software (Wayne Rasband, USA).

Biofilm mass was measured using a protocol described and modified by Delatolla et al. (2008), Ren et al. (2016), Schopf et al. (2018), and Arabgol et al. (2020). Biofilm carriers were harvested from MBBR reactors P_{N1} and P_{N2} and dried at 105°C overnight. Dried carriers were cooled in a desiccator for a minimum of 30 min, after which their weights were recorded as W_1. The dried carriers were then thoroughly cleaned with a stiff-bristled brush and warm water and were dried again at 105°C overnight. The dried carriers were cooled for another 30 min in a desiccator, and their weights were recorded as W_2. The biofilm mass was calculated as the difference between W_1 and

W_2. Prior testing was done to ensure that biofilm removal and heating did not cause any significant change in the mass of the biofilm carrier.

2.5. Cell viability

Biofilm carriers were harvested from each reactor P_{N1} and P_{N2} and cut into sections to expose the inner biofilm surfaces. The sections were stained using a Film Tracer LIVE/DEAD biofilm viability kit (Life Technologies Ontario, Canada), which comprises SYTO 9 stain (a green nucleic acid stain that illuminates the intact cell membrane) and propidium iodide, which only stains cells with damaged cell membranes (i.e., non-viable cells). Calcfluor white stain (Sigma-Aldrich, MO, United States) was used to fluoresce biofilm extracellular polymeric substances (EPS) (Chen et al., 2007). Viable and non-viable embedded cells in the biofilm were observed using a 510/AxioImager confocal laser scanning microscope (CLSM) (Zeiss, VA, United States) equipped with argon and helium-neon lasers with a variety of wavelengths. A minimum of 20 images were acquired at over a depth of 50 μm to determine the number of viable and nonviable cells across the entire biofilm depth. Cell viability based on the CLSM images was determined using NI Vision Assistant 8.0 software (National Instruments, LabView, 2018). The biofilm area was determined and outlined by tracing the calcfluor white stain. The image color threshold on the CLSM images was used to calibrate the area of an identifiable single cell. The standardized images were then used to quantify the biofilm area and the area of viable and non-viable cells (Delatolla et al., 2009; Ren et al., 2016; Ahmed and Delatolla, 2021).

2.6. Quantification of AOB and NOB

2.6.1. DNA extraction

Ammonia-oxidizing bacteria and NOB cell counts were determined using droplet digital PCR (ddPCR). Two carriers each, from reactors P_{N1} and P_{N2}, were collected, and genomic DNA from their biofilms was extracted using a FastDNA*Spin Kit for Soil (MP Biomedicals, CA, United States). The DNA concentrations were analyzed using an Invitrogen Qubit™ 3.0 Fluorometer. Extracted DNA was stored at –80°C until ddPCR analysis.

2.6.2. ddPCR analyses

AOB cell counts were quantified by targeting ammonia monooxygenase subunit A (amoA). The set of amoA primers (*amoA*-1f/*amoA*-2r) targeted a stretch of conserved regions of the known amoA gene sequence of *Nitrosomonas europaea*. Also, two coupled primers, FGPS872f/FGPS1269r and NSR1113f/NSR1264r, were used to amplify the NOB, *Nitrobacter,* and *Nitrospria,* respectively (Table 1; Degrange and Bardin, 1995; Rotthauwe et al., 1997; Geets et al., 2007). The ddPCR mixture was constituted using 5L of sample and 11L of QX200™ ddPCR™ EvaGreen*Supermix (Bio-Ras, Hercules, CA, United States), including 0.23 L of each forward and reverse primer (10 mol/L) and 6.04 L of nuclease-free water. Each ddPCR analysis was performed using a 20 L reaction mixture combined with 65 L of droplet generation oil for EvaGreen to form droplets using a droplet generator. Using a multi-channeled pipette, 40 L of generated droplets were carefully transferred into a 96 well ddPCR plate (Eppendorf,

TABLE 1 Primer details and annealing temperatures.

Target	Primer	Sequence (5′–3′)	Annealing temperature (°C)	Reference
AOB	amoA-1f	GGGGTTTCTACTGGTGGT	53	Rotthauwe et al. (1997)
	amoA-2r	CCCCTCKGSAAAGCCTTCTTC		
NOB – *Nitrobacter*	FGPS872f	CTAAAACTCAAAGGAATTGA	56	Degrange and Bardin (1995)
	FGPS1269r	TTTTTTGAGATTTGCTAG		
NOB – *Nitrospira*	NSR1113f	CCTGCTTTCAGTTGCTACCG	53	Bao et al. (2017)
	NSR1264r	GTTTGCAGCGCTTTGTACCG		

Hamburg, Germany). The plate was sealed using a plate sealer machine and transferred into a T100™ thermal cycler (Bio-Rad, Hercules, CA, United States) for DNA amplification. The amplification program consisted of the following steps: denaturation at 95°C for 5 min, followed by 50 cycles of 30 s at 95°C, 60 s at the corresponding primer annealing temperature (Table 1), and 30 s at 72°C, followed by a 5 min cooldown at 4°C, 5 min at 90°C for droplet stabilization and a hold at 12°C. The QX200 droplet reader (Bio-Rad, Hercules, CA, United States) was applied, and the results were analyzed using QuantaSoft Software (Bio-Rad, version 1.7.4, Hercules. CA, United States). The software measures the number of positive and negative droplets per fluorophore per sample, with each positive counted as a 1 and each negative counted as a 0. The quality control measure ensured that the total droplets quantified were >10,000, and <5 positive droplets were identified as negative controls (Tian et al., 2020).

2.7. Statistical analyses

Statistical analyses of wastewater constituents, biofilm thickness, mass and viable/non-viable cell percentages were determined using the student's *t*-test, with a *value of p* less than 0.05 indicating a significant difference. In addition, the student's *t*-test was used to ascertain statistical significance for the bacterial gene copies with a *value of p* of less than 0.10 considered to indicate a statistically significant difference. Graphical charts and bars were prepared using GraphPad Prism 8.4.1, with error bars in figures being plotted at the 95% confidence intervals (CI).

3. Results and discussion

3.1. Performance of a two-reactor in series partial nitritation MBBR system

The partial nitritation MBBR system, both P_{N1} and P_{N2}, was operated at a target elevated TAN SALR of 5 g TAN/m^2·d and showed steady and stable performance over a 90-day period of operation (Figure 2), with measured SALR values for P_{N1} and P_{N2} 5.07 ± 0.22 and 5.05 ± 0.12 g TAN/m^2·d, respectively. The average TAN surface area removal rate (SARR) of the first reactor, P_{N1}, is 2.25 ± 0.08 g TAN/m^2·d, corresponding to a TAN oxidation efficiency of 45.3 ± 1.1%. The resultant TAN SARR of 2.01 ± 0.07 g TAN/m^2·d from the complete partial nitritation MBBR in series system, P_{N1-N2}, (Figure 2A), corresponds to a TAN oxidation efficiency of 59.7 ± 1.3%. These values

are comparable to the ideal TAN oxidation efficiency of 57%, based on the stoichiometric NO_2^--N: NH_4^+-N molar ratio of 1.32:1 for subsequent anammox treatment (Strous et al., 1997; Van Dongen et al., 2001). The observed TAN oxidation efficiency from the partial nitritation MBBR system, P_{N1-N2}, is also similar to the TAN oxidation efficiency of 60% previously reported in the mainstream partial nitritation MBBR system while utilizing a combination of DO/TAN ratio control and FA inhibition as control strategies (Kowalski et al., 2019b). However, the current elevated loading, two-reactor in series design strategy herein studied does not require operational control while demonstrating robust and steady performance.

The percent NO_x as nitrite was monitored in the partial nitritation MBBR system over a period of 90 days and demonstrates stable and steady performance (Figure 2B). The P_{N1} and P_{N2} reactors show an average percent NO_x as nitrite of 81.2 ± 2.1 and 74.7 ± 0.9%, respectively. The average percent NO_x as nitrite of the total oxidized TAN from the partial nitritation MBBR system, P_{N1-N2}, indicates that partial nitritation was achieved, i.e., TAN was oxidized to nitrite and oxidation of nitrite to nitrate was largely mitigated. The relative nitrate production varied between 13 and 16% in the reactors P_{N1} and P_{N2}. Similar levels of relative nitrate production have also been reported in mainstream partial nitritation and single-stage PN/A MBBR systems (Gilbert et al., 2014; Persson et al., 2017; Gu et al., 2018; Gustavsson et al., 2020). Therefore, the minimal levels of nitrate build-up in the elevated loaded partial nitritation MBBR system suggest that the NOB population in the biofilm or the NOB activity of the embedded population are possibly suppressed.

Finally, the average effluent TAN, nitrite, and nitrate concentrations from reactor P_{N1} of 20.1 ± 1.30 mg TAN/L, 7.14 ± 0.81 mg NO_2^--N/L, and 4.02 ± 0.21 mg NO_3^--N/L demonstrate a NO_2^--N:NH_4^+-N stoichiometric ratio of 0.36:1 (Figure 3). This stoichiometric ratio from reactor P_{N1} is below the ideal metabolic ratio of 1.32:1 for partial nitritation systems upstream of anammox systems. From a practical standpoint, a stoichiometric ratio near 1:1 has also been reported sufficient for mainstream anammox operation in an MBBR system (Gu et al., 2018). Therefore, with the introduction of the second reactor (P_{N2}) in series to the first reactor (P_{N1}) in this study, the average effluent TAN, nitrite, and nitrate concentrations of 12.9 ± 1.84 mg TAN/L, 13.9 ± 1.56 mg NO_2^--N/L and 3.11 ± 0.29 mg NO_3^--N/L, were measured respectively. These P_{N2} effluent concentrations correspond to a metabolic ratio of 1.15:1. As such, this ratio provides suitable nitrogen speciation for the subsequent downstream anammox treatment, and the two-reactors in series partial nitritation MBBR system configuration in this study herein provides a stable effluent quality for subsequent downstream anammox operation.
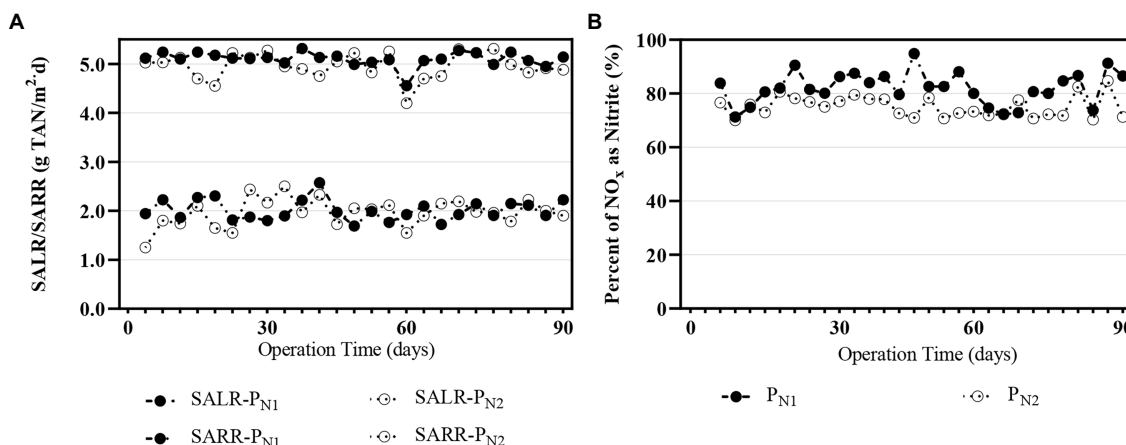
FIGURE 2
Performance of partial nitritation MBBR system **(A)** SALR/SARR over time P_{N1} and P_{N2} **(B)** percent NO_x as nitrite over time for P_{N1} and P_{N2}.
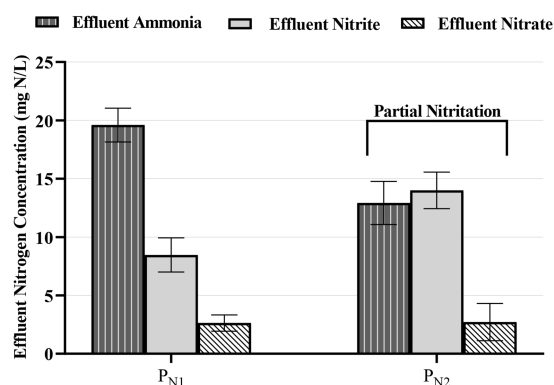

FIGURE 3
Effluent TAN (vertical shading), nitrite (solid light gray fill), and nitrate (diagonal shading) concentrations in the partial nitritation MBBR system, P_{N1} and P_{N2} (average±95%CI).
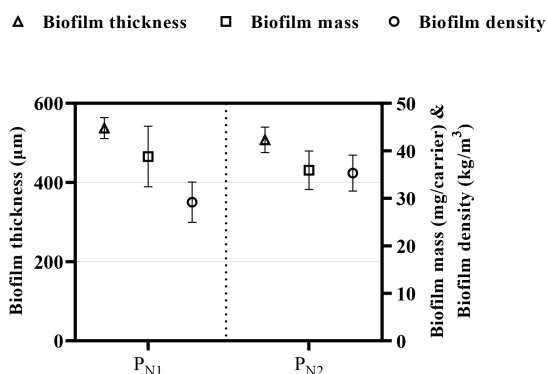

FIGURE 4
Biofilm thickness (triangle), biofilm mass (square), and biofilm density (circle), for partial nitritation MBBR system, P_{N1}, and P_{N2} (average±95% CI).

3.2. Biofilm characteristics and morphology

The meso-scale effects of the elevated TAN SALR on the biofilm were quantified through the analysis of biofilm characteristics described as biofilm thickness, biofilm mass, biofilm density, and morphology (Figure 4). The biofilm thickness is 577 ± 21 and $517 \pm 43\,\mu m$; the biofilm mass is 38.8 ± 1.2 and $35.5 \pm 3.1\,mg/carrier$ corresponding to biofilm density (calculated based on biofilm thickness and biofilm mass) of 29.9 ± 9.2 and $33.7 \pm 8.7\,kg/m^3$ in the P_{N1} and P_{N2} reactors, respectively. The average biofilm thickness of $547 \pm 65\,\mu m$ in the partial nitritation MBBR system (P_{N1} and P_{N2}) is higher than the $300\,\mu m$ reported in the mainstream partial nitritation MBBR system (Piculell et al., 2016b,c). The difference in biofilm thickness could be expected as the carrier type and control strategy utilized in both studies are different and would result in varying biofilm composition or characteristics. However, the biofilm thickness, mass, and density are within the range reported in a previous study on elevated loaded partial nitritation MBBR systems with comparable operational conditions (Schopf et al., 2021).

On the other hand, the qualitative assessment of the biofilm shape and morphology shows a rough, irregular, and thick biofilm. This finding is consistent with previous studies showing thick biofilms at similar elevated TAN SALR of $5\,g\ TAN/m^2 \cdot d$ in a partial nitritation MBBR system (Schopf et al., 2019). The thick biofilm is possible as elevated loading conditions and high substrate load allow for a deeper substrate penetration into the biofilm, supporting high cell growth. Furthermore, previous studies have demonstrated that increased biofilm thickness leads to steep substrate gradients and stratification of the metabolic process throughout the biofilm, likely resulting in a more biodiverse and heterogeneous biofilm, thus potentially influencing the overall performance of the system (Torresi et al., 2016; Suarez et al., 2019). Therefore, the stable and steady partial nitritation performance observed in this study at elevated TAN SALR could be explained by stratification that occurs in thick biofilms with AOB population dominating the upper layers of the biofilm and NOB population at deeper layers as the system operates under DO mass transfer rate limited conditions (Pérez et al., 2014; Malovanyy et al.,

2015). As such, NOB population or activity is likely suppressed due to the limited diffusion of DO in the biofilm of elevated loading partial nitritation MBBR system of the herein study.

3.3. Cell viability

In an MBBR system, the higher substrate removal rate can be related to live cells or biomass activities on the carrier (Ødegaard, 2006), and as such, the biomass embedded in the biofilm controls the reactor performance. Biofilm structure, in general, and within the MBBR system, typically consists of viable cells and non-viable bacterial cells (Figure 5) along with numerous other substances secreted by the cells and attached substances to the extracellular matrix of the biofilm. The total cell viability (%) ranges from 58.5 to 99.9% in P_{N1} and from 45.8 to 97.1% in the P_{N2} reactor (Figure 5A). Although total cell viability is likely affected by residual TAN concentration and specific embedded microbial communities, the live fraction of total cells, which is the ratio of live cells and the total number of cells (viable + non-viable cells), is stable (Figures 5B,C) and within conventional range in a nitrifying MBBR system (Young et al., 2017a). Hence, the viability of the cells does not appear to constrain the performance of the elevated loaded partial nitritation MBBR reactors, and the mainstream elevated loaded partial nitritation MBBR system retained carriers with viable embedded biomass to maintain sufficient microbial activities for stable and steady partial nitritation performance.
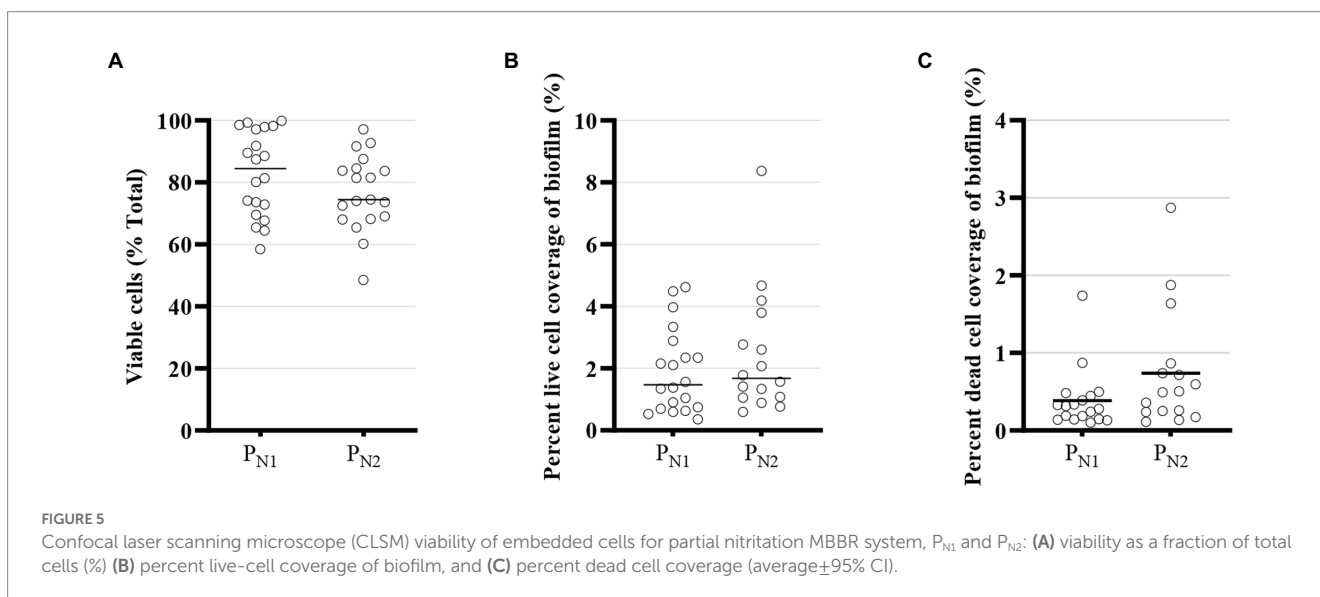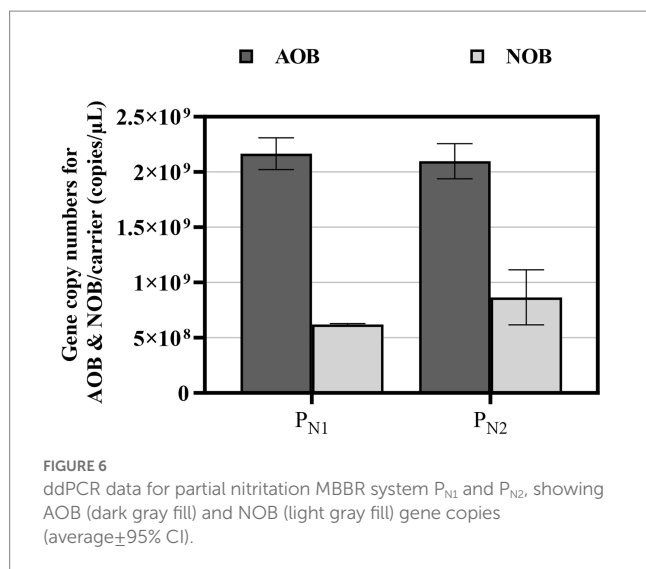
3.4. Quantification of AOB and NOB

The copies of AOB and NOB were quantified in the partial nitritation MBBR reactors P_{N1} and P_{N2} using ddPCR (Figure 6). In mainstream partial nitritation reactors, the low bulk nitrite concentration would likely select for *Nitrospira* rather than *Nitrobacter* due to its high substrate affinity (Wang et al., 2019). As such, *Nitrospira* was the only NOB detected in the reactors P_{N1} and P_{N2}. During the

stable and steady partial nitritation, the average gene copy numbers of AOB are $1.92 \pm 3.40 \times 10^9$ and $2.02 \pm 2.51 \times 10^9$ copies/carrier, and the average gene copy numbers of NOB are $6.20 \pm 1.55 \times 10^8$ and $1.15 \pm 1.20 \times 10^9$ copies/carrier, in reactor P_{N1} and P_{N2}, respectively. These average AOB and NOB, gene copy numbers are statistically similar and correspond to AOB to NOB ratios of 3.21:1 and 2.12:1 in reactors P_{N1} and P_{N2}, respectively. These low ratios are comparable to a single mainstream PN/A MBBR system (Gilbert et al., 2015). Also, these values are higher than those published from full nitrification conventional suspended growth systems by Limpiyakorn et al. (2005) and Yao and Peng (2017), and full nitrification MBBR system by Zhang et al. (2019). However, these AOB to NOB ratios are lower than those reported in partial nitritation, conventional suspended growth, and MBBR systems operated under elevated TAN concentrations (Abzazou et al., 2016; Zhang et al., 2020). This distinction in AOB to NOB ratios in full nitrification and partial nitritation systems is possible due to varying reactor types and experimental and operational conditions. Therefore, in the study, the elevated loaded partial nitritation MBBR system demonstrates that NOB activity suppression is the likely dominant mechanism responsible for stable and steady partial nitritation performance under mainstream conditions.

3.5. The mechanism of nitrite oxidation suppression in the mainstream partial nitritation MBBR system

To determine the mechanism of nitrite oxidation suppression caused by the low operational intensity partial nitritation design strategy, the driving hypothesis is that elevated TAN SALR and the resulting impact on the biofilm morphology will play a key role in suppressing NOB population or activity in the partial nitritation MBBR system. Previous studies have suggested that the steep substrate gradient present in the biofilm and competition for DO between AOB and NOB, acts as the main mechanism for the control of NOB population or activity in a biofilm-based system (Brockmann and Morgenroth, 2008; Pérez et al., 2014; Isanta et al.,

FIGURE 5
Confocal laser scanning microscope (CLSM) viability of embedded cells for partial nitritation MBBR system, P_{N1} and P_{N2}: **(A)** viability as a fraction of total cells (%) **(B)** percent live-cell coverage of biofilm, and **(C)** percent dead cell coverage (average $\pm$ 95% CI).

FIGURE 6
ddPCR data for partial nitritation MBBR system P_{N1} and P_{N2}, showing AOB (dark gray fill) and NOB (light gray fill) gene copies (average$\pm$95% CI).

2015; Laureni et al., 2016). This is possible as external mass transfer boundary layer controls the movement of the substrate (TAN) or the electron acceptor (DO) and determines the actual TAN or DO concentration at the biofilm surface (Brockmann and Morgenroth, 2008; Pérez et al., 2014; Isanta et al., 2015; Laureni et al., 2016). The resultant mass transfer limitations (DO mass transfer limited condition) have been numerically demonstrated to promote the suppression of NOB in a partial nitritation MBBR system (Pérez et al., 2020).

Therefore, in this study, elevated TAN SALR and resulting morphological impact on biofilm is the main factor that could be possibly controlling NOB activity suppression rather than NOB population suppression. At elevated TAN SALR, AOB possibly has a higher competitive advantage over NOB due to the high TAN concentration in the bulk solution resulting from elevated TAN SALR, which results in DO being preferentially consumed by AOB compared to NOB. Moreover, elevated TAN SALR, in addition to the resultant biofilm thickness and morphology (roughness), builds an increased mass transfer resistance that possibly limits the mass transfer of oxygen from the bulk solution into the biofilm, resulting in limited DO uptake by NOB and subsequently suppressing their activity. Hence, by maintaining significant AOB activity and suppressing NOB activity, the MBBR system achieves 59.7% TAN oxidation efficiency and, thus, a $NO_2^--N:NH_4^+-N$ stoichiometric ratio of 1.15:1 with $83.2 \pm 1.2\%$ percent of NO_x as nitrite.

3.6. The implications of the study

The study shows that an elevated loading design strategy, as opposed to operational control strategies, is able to achieve stable, steady, and robust partial nitritation in an MBBR system under mainstream municipal conditions. The finding from this study provides a feasible design strategy that does not require multiple and complex operational control measures or monitoring, to achieve stable and steady partial nitritation. The operation at elevated TAN SALR and the resulting impact on biofilm morphology essentially restricts DO uptake by NOB, which is beneficial to the long-term

suppression of their activity. Therefore, elevated TAN SALR allows for effective NOB suppression that could result in long-term process stability and stable effluent quality for the subsequent downstream anammox treatment at mainstream municipal wastewater. The design strategy is herein demonstrated at the laboratory scale with synthetic wastewater; hence, the elevated TAN SALR strategy requires further investigation at the pilot scale using real wastewater with the potential to guide future implementation of a high-rate, compact, and low-operational intensive partial nitritation system at WRRFs.

In addition, regarding the future of the elevated loaded partial nitritation system following an anammox system as a two-stage configuration for effective nitrogen removal at mainstream municipal wastewater. Successful anammox operation as a two-stage PN/A system is achievable if operated with stable and steady partial nitritation effluent as well as an appropriate $NO_2^--N:NH_4^+-N$ metabolic ratio. According to the results from this study, the elevated loaded partial nitritation MBBR system is robust, effective, stable, steady and can maintain appropriate effluent ratios. As such, anammox enrichment and operation under mainstream conditions is feasible with the possibility of achieving high nitrogen removal rates and long-term process stability. Also, designing the partial nitritation MBBR system at an elevated TAN loading rate allows for high rate partial nitritation and, consequently, a small land footprint. Therefore, the introduction of the combined two-stage PN/A system can be achieved where insufficient land availability exists. On this note, further studies are proposed exploring the elevated loaded partial nitritation MBBR system as a two-stage PN/A system for enhanced nitrogen removal from mainstream municipal wastewaters.

4. Conclusion

The two-reactor in series elevated loaded mainstream partial nitritation MBBR system achieves stable and steady partial nitritation with an effluent $NO_2^--N:NH_4^+-N$ concentration corresponding to a molar stoichiometric ratio of 1.15:1. Hence, demonstrating possible suitable nitrogen speciation for the subsequent downstream anammox treatment. The biofilm thickness and morphology in the reactors show thick biofilms with the embedded biomass showing no viability constraint, as the embedded cells remained viable, supporting the observed stable and steady partial nitritation performance. The thick biofilm morphology likely reduced the diffusive transport of DO into the biofilm, that limits the DO uptake by NOB population. The AOB and NOB gene copy numbers of the MBBR biofilm show that rather than NOB population suppression, NOB activity suppression is the likely mechanism responsible for the stable and steady partial nitritation performance in the mainstream elevated loaded partial nitritation MBBR system.

Data availability statement

The original contributions presented in the study are included in the article/supplementary material, further inquiries can be directed to the corresponding author.

Author contributions

JI contributed to the conception and design of the study, performed the research, analyzed the data, and wrote the manuscript. HC contributed to data acquisition and analysis. RD developed the research questions and experimental design, supervised, and coordinated the research, reviewed the manuscript, and acquired funding for the research. All authors contributed to the article and approved the submitted version.

Acknowledgments

Conflict of interest

The authors declare that the research was conducted in the absence of any commercial or financial relationships that could be construed as a potential conflict of interest.

Publisher's note

All claims expressed in this article are solely those of the authors and do not necessarily represent those of their affiliated organizations, or those of the publisher, the editors and the reviewers. Any product that may be evaluated in this article, or claim that may be made by its manufacturer, is not guaranteed or endorsed by the publisher.

References

Abzazou, T., Araujo, R. M., Auset, M., and Salvadó, H. (2016). Tracking and quantification of nitrifying bacteria in biofilm and mixed liquor of a partial nitrification MBBR pilot plant using fluorescence in situ hybridization. *Sci. Total Environ.* 541, 1115–1123. doi: 10.1016/j.scitotenv.2015.10.007

Agrawal, S., Seuntjens, D., De Cocker, P., Lackner, S., and Vlaeminck, S. E. (2018). Success of mainstream partial nitration/anammox demands integration of engineering, microbiome and modeling insights. *Curr. Opin. Biotechnol.* 50, 214–221. doi: 10.1016/j.copbio.2018.01.013

Ahmed, W., and Delatolla, R. (2021). Biofilm and microbiome response of attached growth nitrification systems across incremental decreases to low temperatures. *J. Water Process Eng.* 39:101730. doi: 10.1016/j.jwpe.2020.101730

Arabgol, R., Vanrolleghem, P. A., Piculell, M., and Delatolla, R. (2020). The impact of biofilm thickness-restraint and carrier type on attached growth system performance, solids characteristics and settleability. *Environ. Sci. Water Res. Technol.* 6, 2843–2855. doi: 10.1039/d0ew00314j

Bao, P., Wang, S., Ma, B., Zhang, Q., and Peng, Y. (2017). Achieving partial nitrification by inhibiting the activity of Nitrospira-like bacteria under high-DO conditions in an intermittent aeration reactor. *Journal of Environmental Sciences* 56, 71–78. doi: 10.1016/j.jes.2016.09.004

Brockmann, D., and Morgenroth, E., (2008). Partial nitrification in biofilms: Inhibition versus competition. Presented at the Outline paper for IWA world water congress.

Chen, M.-Y., Lee, D.-J., Tay, J.-H., and Show, K.-Y. (2007). Staining of extracellular polymeric substances and cells in bioaggregates. *Appl. Microbiol. Biotechnol.* 75, 467–474. doi: 10.1007/s00253-006-0816-5

Chen, R., Takemura, Y., Liu, Y., Ji, J., Sakuma, S., Kubota, K., et al. (2018). Using partial nitrification and anammox to remove nitrogen from low-strength wastewater by co-immobilizing biofilm inside a moving bed bioreactor. *ACS Sustain. Chem. Eng.* 7, 1353–1361. doi: 10.1021/acssuschemeng.8b05055

Choi, D., and Jung, J. (2022). Evaluation of operating parameters affecting the two-stage nitritatin/anammox process in mainstream flows: from lab-scale to pilot-scale. *J. Biosci. Bioeng.* 134, 48–54. doi: 10.1016/j.jbiosc.2022.04.005

Clesceri, L. S., Greenberg, A., and Eaton, A. D. (1999). *Standard methods for the examination of water and wastewater. 20th* Edn American Water Work Association, Water Environment Federation, Washington, DC. APHA-AWWA-WEF.

Degrange, V., and Bardin, R. (1995). Detection and counting of Nitrobacter populations in soil by PCR. *Appl. Environ. Microbiol.* 61, 2093–2098. doi: 10.1128/aem.61.6.2093-2098.1995

Delatolla, R., Berk, D., and Tufenkji, N. (2008). Rapid and reliable quantification of biofilm weight and nitrogen content of biofilm attached to polystyrene beads. *Water Res.* 42, 3082–3088. doi: 10.1016/j.watres.2008.02.023

Delatolla, R., Tufenkji, N., Comeau, Y., Gadbois, A., Lamarre, D., and Berk, D. (2009). Kinetic analysis of attached growth nitrification in cold climates. *Water Sci. Technol.* 60, 1173–1184. doi: 10.2166/wst.2009.419

Geets, J., De Cooman, M., Wittebolle, L., Heylen, K., Vanparys, B., De Vos, P., et al. (2007). Real-time PCR assay for the simultaneous quantification of nitrifying and denitrifying bacteria in activated sludge. *Appl. Microbiol. Biotechnol.* 75, 211–221. doi: 10.1007/s00253-006-0805-8

Gilbert, E. M., Agrawal, S., Karst, S. M., Horn, H., Nielsen, P. H., and Lackner, S. (2014). Low temperature partial nitration/anammox in a moving bed biofilm reactor treating low strength wastewater. *Environ. Sci. Technol.* 48, 8784–8792. doi: 10.1021/es501649m

Gilbert, E. M., Agrawal, S., Schwartz, T., Horn, H., and Lackner, S. (2015). Comparing different reactor configurations for partial nitration/anammox at low temperatures. *Water Res.* 81, 92–100. doi: 10.1016/j.watres.2015.05.022

Gu, J., Yang, Q., and Liu, Y. (2018). Mainstream anammox in a novel A-2B process for energy-efficient municipal wastewater treatment with minimized sludge production. *Water Res.* 138, 1–6. doi: 10.1016/j.watres.2018.02.051

Gustavsson, D. J., Suarez, C., Wilén, B.-M., Hermansson, M., and Persson, F. (2020). Long-term stability of partial nitration-anammox for treatment of municipal wastewater in a moving bed biofilm reactor pilot system. *Sci. Total Environ.* 714:136342. doi: 10.1016/j.scitotenv.2019.136342

Hem, L. J., Rusten, B., and Ødegaard, H. (1994). Nitrification in a moving bed biofilm reactor. *Water Res.* 28, 1425–1433. doi: 10.1016/0043-1354(94)90310-7

Hoekstra, M., Geilvoet, S. P., Hendrickx, T. L., van Erp Taalman Kip, C. S., Kleerebezem, R., and van Loosdrecht, M. C. M. (2019). Towards mainstream anammox: lessons learned from pilot-scale research at WWTP Dokhaven. *Environ. Technol.* 40, 1721–1733. doi: 10.1080/09593330.2018.1470204

Ikem, J., Schopf, A., Chen, H., and Delatolla, R. (2023). Optimized design of a stable, long term and robust attached growth mainstream partial nitration system. Available at: https://engrxiv.org/preprint/view/2770/5175 (Accessed January 4, 2023).

Isanta, E., Reino, C., Carrera, J., and Pérez, J. (2015). Stable partial nitration for low-strength wastewater at low temperature in an aerobic granular reactor. *Water Res.* 80, 149–158. doi: 10.1016/j.watres.2015.04.028

Kowalski, M. S., Devlin, T. R., di Biase, A., and Oleszkiewicz, J. A. (2019a). Effective nitrogen removal in a two-stage partial nitration-anammox reactor treating municipal wastewater–piloting PN-MBBR/AMX-IFAS configuration. *Bioresour. Technol.* 289:121742. doi: 10.1016/j.biortech.2019.121742

Kowalski, M. S., Devlin, T. R., di Biase, A., and Oleszkiewicz, J. A. (2019b). Controlling cold temperature partial nitration in moving bed biofilm reactor. *Chemosphere* 227, 216–224. doi: 10.1016/j.chemosphere.2019.04.025

Lackner, S., Gilbert, E. M., Vlaeminck, S. E., Joss, A., Horn, H., and van Loosdrecht, M. C. (2014). Full-scale partial nitration/anammox experiences–an application survey. *Water Res.* 55, 292–303. doi: 10.1016/j.watres.2014.02.032

Laureni, M., Falås, P., Robin, O., Wick, A., Weissbrodt, D. G., Nielsen, J. L., et al. (2016). Mainstream partial nitration and anammox: long-term process stability and effluent quality at low temperatures. *Water Res.* 101, 628–639. doi: 10.1016/j.watres.2016.05.005

Laureni, M., Weissbrodt, D. G., Villez, K., Robin, O., De Jonge, N., Rosenthal, A., et al. (2019). Biomass segregation between biofilm and flocs improves the control of nitrite-oxidizing bacteria in mainstream partial nitration and anammox processes. *Water Res.* 154, 104–116. doi: 10.1016/j.watres.2018.12.051

Li, X., Klaus, S., Bott, C., and He, Z. (2018). Status, challenges, and perspectives of mainstream Nitritation–Anammox for wastewater treatment. *Water Environ. Res.* 90, 634–649. doi: 10.2175/106143017X15131012153112

Limpiyakorn, T., Shinohara, Y., Kurisu, F., and Yagi, O. (2005). Communities of ammonia-oxidizing bacteria in activated sludge of various sewage treatment plants in Tokyo. *FEMS Microbiol. Ecol.* 54, 205–217. doi: 10.1016/j.femsec.2005.03.017

Lotti, T., Kleerebezem, R., Hu, Z., Kartal, B., Jetten, M., Van Loosdrecht, M. (2014). Simultaneous partial nitration and anammox at low temperature with granular sludge. *Water Research* 66, 111–121. doi: 10.1016/j.watres.2014.07.047

Lotti, T., Kleerebezem, R., Abelleira-Pereira, J., Abbas, B., and Van Loosdrecht, M. (2015a). Faster through training: the anammox case. *Water Res.* 81, 261–268. doi: 10.1016/j.watres.2015.06.001

Lotti, T., Kleerebezem, R., Hu, Z., Kartal, B., de Kreuk, M. K., van Erp Taalman Kip, C., et al. (2015b). Pilot-scale evaluation of anammox-based mainstream nitrogen removal from municipal wastewater. *Environ. Technol.* 36, 1167–1177. doi: 10.1080/09593330.2014.982722

Malovanyy, A., Yang, J., Trela, J., and Plaza, E. (2015). Combination of upflow anaerobic sludge blanket (UASB) reactor and partial nitritation/anammox moving bed biofilm reactor (MBBR) for municipal wastewater treatment. *Bioresour. Technol.* 180, 144–153. doi: 10.1016/j.biortech.2014.12.101

Odegaard, H. (1999). *The Moving Bed Biofilm Reactor. Water Environmental Engineering and Reuse of Water* Hokkaido Press, 250–305.

Ødegaard, H. (2006). Innovations in wastewater treatment:–the moving bed biofilm process. *Water Sci. Technol.* 53, 17–33. doi: 10.2166/wst.2006.284

Pedrouso, A., Trela, J., Val del Rio, A., Mosquera-Corral, A., and Plaza, E. (2019). Performance of partial nitritation-anammox processes at mainstream conditions in an IFAS system. *J. Environ. Manage.* 250:109538. doi: 10.1016/j.jenvman.2019.109538

Pérez, J., Laureni, M., van Loosdrecht, M. C., Persson, F., and Gustavsson, D. J. (2020). The role of the external mass transfer resistance in nitrite oxidizing bacteria repression in biofilm-based partial nitritation/anammox reactors. *Water Res.* 186:116348. doi: 10.1016/j.watres.2020.116348

Pérez, J., Lotti, T., Kleerebezem, R., Picioreanu, C., and van Loosdrecht, M. C. (2014). Outcompeting nitrite-oxidizing bacteria in single-stage nitrogen removal in sewage treatment plants: a model-based study. *Water Res.* 66, 208–218. doi: 10.1016/j.watres.2014.08.028

Persson, F., Suarez, C., Hermansson, M., Plaza, E., Sultana, R., and Wilén, B. (2017). Community structure of partial nitritation-anammox biofilms at decreasing substrate concentrations and low temperature. *Microb. Biotechnol.* 10, 761–772. doi: 10.1111/1751-7915.12435

Piculell, M., Christensson, M., Jönsson, K., and Welander, T. (2016a). Partial nitritation in MBBRs for mainstream deammonification with thin biofilms and alternating feed supply. *Water Sci. Technol.* 73, 1253–1260. doi: 10.2166/wst.2015.599

Piculell, M., Suarez, C., Li, C., Christensson, M., Persson, F., Wagner, M., et al. (2016b). The inhibitory effects of reject water on nitrifying populations grown at different biofilm thickness. *Water Res.* 104, 292–302. doi: 10.1016/j.watres.2016.08.027

Piculell, M., Welander, P., Jönsson, K., and Welander, T. (2016c). Evaluating the effect of biofilm thickness on nitrification in moving bed biofilm reactors. *Environ. Technol.* 37, 732–743. doi: 10.1080/09593330.2015.1080308

Ren, B., Young, B., Variola, F., and Delatolla, R. (2016). Protein to polysaccharide ratio in EPS as an indicator of non-optimized operation of tertiary nitrifying MBBR. *Water Qual. Res. J. Can.* 51, 297–306. doi: 10.2166/wqrjc.2016.040

Rotthauwe, J.-H., Witzel, K.-P., and Liesack, W. (1997). The ammonia monooxygenase structural gene amoA as a functional marker: molecular fine-scale analysis of natural ammonia-oxidizing populations. *Appl. Environ. Microbiol.* 63, 4704–4712. doi: 10.1128/aem.63.12.4704-4712.1997

Schopf, A., Delatolla, R., and Kirkwood, K. M. (2019). Partial nitritation at elevated loading rates: design curves and biofilm characteristics. *Bioprocess Biosyst. Eng.* 42, 1809–1818. doi: 10.1007/s00449-019-02177-8

Schopf, A., Delatolla, R., Mathew, R., Tsitouras, A., and Kirkwood, K. M. (2018). Investigation of copper inhibition of nitrifying moving bed biofilm (MBBR) reactors during long term operations. *Bioprocess Biosyst. Eng.* 41, 1485–1495. doi: 10.1007/s00449-018-1976-2

Schopf, A., Kirkwood, K. M., Tsitouras, A., and Delatolla, R. (2021). Elevated loading rates as a low operational intensity and small land footprint design strategy to achieve partial nitritation. *J. Water Process Eng.* 44:102381. doi: 10.1016/j.jwpe.2021.102381

Schraa, O., Rosenthal, A., Wade, M., Rieger, L., Miletić, I., and Alex, J. (2020). Assessment of aeration control strategies for biofilm-based partial nitritation/anammox systems. *Water Sci. Technol.* 81, 1757–1765. doi: 10.2166/wst.2020.174

Stefansdottir, D., Christensson, M., and Piculell, M., (2015). Process description for maintaining stable nitrogen removal using nitritation + anammox with MBBRs in mainstream water. Project report deliverable no. 2.3. POWERSTEP. European Union http://www.powerstep.eu/system/files/generated/files/resource/d2-3-process-description-for-maintaining-stable-nitrogen-removal-using-nitritation-anammox.pdf (Accessed February 15, 2023).

Strous, M., Heijnen, J., Kuenen, J. G., and Jetten, M. (1998). The sequencing batch reactor as a powerful tool for the study of slowly growing anaerobic ammonium-oxidizing microorganisms. *Appl. Microbiol. Biotechnol.* 50, 589–596. doi: 10.1007/s002530051340

Strous, M., Van Gerven, E., Zheng, P., Kuenen, J. G., and Jetten, M. S (1997). Ammonium removal from concentrated waste streams with the anaerobic ammonium oxidation (anammox) process in different reactor configurations. *Water Research* 31, 1955–1962. doi: 10.1016/S0043-1354(97)00055-9

Suarez, C., Piculell, M., Modin, O., Langenheder, S., Persson, F., and Hermansson, M. (2019). Thickness determines microbial community structure and function in nitrifying biofilms via deterministic assembly. *Sci. Rep.* 9, 1–10. doi: 10.1038/s41598-019-41542-1

Tian, X., Ahmed, W., and Delatolla, R. (2019). Nitrifying bio-cord reactor: performance optimization and effects of substratum and air scouring. *Environ. Technol.* 40, 480–488. doi: 10.1080/09593330.2017.1397760

Tian, X., Schopf, A., Amaral-Stewart, B., Christensson, M., Morgan-Sagastume, F., Vincent, S., et al. (2020). Anammox attachment and biofilm development on surface-modified carriers with planktonic-and biofilm-based inoculation. *Bioresour. Technol.* 317:124030. doi: 10.1016/j.biortech.2020.124030

Torresi, E., Fowler, S. J., Polesel, F., Bester, K., Andersen, H. R., Smets, B. F., et al. (2016). Biofilm thickness influences biodiversity in nitrifying MBBRs implications on micropollutant removal. *Environ. Sci. Technol.* 50, 9279–9288. doi: 10.1021/acs.est.6b02007

Trojanowicz, K., Trela, J., and Plaza, E. (2021). Possible mechanism of efficient mainstream partial nitritation/anammox (PN/a) in hybrid bioreactors (IFAS). *Environ. Technol.* 42, 1023–1037. doi: 10.1080/09593330.2019.1650834

Van Dongen, U., Jetten, M. S., and Van Loosdrecht, M. (2001). The SHARON®-Anammox® process for treatment of ammonium rich wastewater. *Water science and Technology* 44, 153–160. doi: 10.2166/wst.2001.0037

Wang, H., Xu, G., Qiu, Z., Zhou, Y., and Liu, Y. (2019). NOB suppression in pilot-scale mainstream nitritation-denitritation system coupled with MBR for municipal wastewater treatment. *Chemosphere* 216, 633–639. doi: 10.1016/j.chemosphere.2018.10.187

Yao, Q., and Peng, D.-C. (2017). Nitrite oxidizing bacteria (NOB) dominating in nitrifying community in full-scale biological nutrient removal wastewater treatment plants. *AMB Express* 7, 1–11. doi: 10.1186/s13568-017-0328-y

Young, B., Delatolla, R., Abujamel, T., Kennedy, K., Laflamme, E., and Stintzi, A. (2017a). Rapid start-up of nitrifying MBBRs at low temperatures: nitrification, biofilm response and microbiome analysis. *Bioprocess Biosyst. Eng.* 40, 731–739. doi: 10.1007/s00449-017-1739-5

Young, B., Delatolla, R., Kennedy, K., Laflamme, E., and Stintzi, A. (2017b). Low temperature MBBR nitrification: microbiome analysis. *Water Res.* 111, 224–233. doi: 10.1016/j.watres.2016.12.050

Zhang, D., Su, H., Antwi, P., Xiao, L., Liu, Z., and Li, J. (2020). High-rate partial-nitrition and efficient nitrifying bacteria enrichment/out-selection via pH-DO controls: efficiency, kinetics, and microbial community dynamics. *Sci. Total Environ.* 692, 741–755. doi: 10.1016/j.scitotenv.2019.07.308

Zhang, M., Yu, M., Wang, Y., He, C., Pang, J., and Wu, J. (2019). Operational optimization of a three-stage nitrification moving bed biofilm reactor (NMBBR) by obtaining enriched nitrifying bacteria: nitrifying performance, microbial community, and kinetic parameters. *Sci. Total Environ.* 697:134101. doi: 10.1016/j.scitotenv.2019.134101